Available online at www.sciencedirect.com

SCIENCE DIRECT®

ELSEVIER

Journal of Magnetism and Magnetic Materials 257 (2003) 79–86

journal of magnetism and magnetic materials

www.elsevier.com/locate/jmmm

Magnetic properties of nano-crystalline Gd- or Pr-substituted $CoFe_2O_4$ synthesized by the citrate precursor technique

R.N. Panda[a], J.C. Shih[b], T.S. Chin[b,c,*]

[a] *Max-plank institute fur Kohlenforschung, Kaiser-Wilheim-platz1, 45470 Mulheim an der Ruhr, Germany*

[b] *Department of Materials Science and Engineering, National Tsing Hua University, 101 Sec 2, Kuang Fu Road, Hsinchu 30043, Taiwan*

[c] *National Lien-Ho Institute of Technology, 360 Miaoli, Taiwan, ROC*

Received 18 April 2002; received in revised form 20 August 2002

Abstract

The magnetic properties of nano-crystalline $CoM_xFe_{2-x}O_4$ (where M = Gd and Pr and $x = 0$, 0.1 and 0.2) powders prepared by a citrate precursor technique have been studied by using vibrating sample magnetometer (VSM). The crystallite sizes of the materials were varied by altering the synthetic conditions and are within the range of a minimum of 6.8 nm and a maximum of 87.5 nm. The materials were characterized by powder X-ray diffraction (XRD) and thermogravimetric (TG) measurements. TG study indicates the formation of the spinel ferrite phase at 220°C. The phase identification of the materials by XRD reveals the single-phase nature of the materials. The room temperature saturation magnetization of the ferrite materials decreases with the reduction of size. This has been attributed to the presence of superparamagnetic fractions in the materials and spin canting at the surface of nano-particles. Insertion of rare-earth atoms in the crystal lattice inhibits the grain growth of the materials in a systematic manner compared with that of the pure cobalt ferrite materials. The improved coercivity compared with those for the pure cobalt ferrites is attributed to the contribution from the single ion anisotropy of the rare-earth ions present in the crystal lattice and the surface effects resulting in alteration of magnetic structures on the surface of nano-particles.

PACS: 75.50.Gg; 75.50.Tt; 75.50.Vv

Keywords: Nanocrystalline; Coercivity; Ferrite; Citrate precursor; X-ray diffraction

1. Introduction

The magnetic behavior of fine particles is of considerable interest both from a scientific and practical point of view [1,2]. This is due to both size and surface effects. The major size effects involve the reduction of domain boundaries, which leads to single-domain particles, and a thermal randomization of the total spin system, commonly denoted as superparamagnetism. The phenomena originating from surface effects include canted spin structures, and magnetic 'dead layers' at surfaces. In small particles, the saturation magnetization (M_s), magnetocrystalline anisotropy (K), Curie

*Corresponding author. Department of Materials Science and Engineering, National Tsing Hua University, 101 Sec 2, Kuang Fu Road, Hsinchu 30043, Taiwan. Tel.: +886-03-571-19035; fax: +886-03-572-2366.

E-mail address: tschin@mse.nthu.edu.tw (T.S. Chin).

0304-8853/03/$ - see front matter
PII: S0304-8853(02)01036-3

temperature (T_c), magnetic hyperfine field (ΔH) and coercivity (H_c) values are found to differ from their bulk behavior [3,4]. In addition, in the understanding of the magnetic relaxation of assemblies of small magnetic particles [5,6], which exhibit a distribution of energy barriers arising from a particle volume distribution, anisotropy field distribution, the role of the interparticle interaction needs to be taken into account. This is particularly true for the enhancement of the lowest energy barrier, which occurs when the dipolar interparticle interactions are controlled by demagnetizing effects and are relevant for the so-called quantum tunneling of the magnetization. Experiments on spin-polarized tunneling between a ferromagnet and a superconductor suggest the possibility of the magnetic field dependence tunneling between two ferromagnets separated by a thin insulator [7].

Despite a large number of studies being available in the literature for understanding of the magnetic phenomena of nano-particles, a conclusive understanding is hampered by the lack of suitable methodology for preparation of nano-sized particles and their narrow distributions. Most of the studies are focused on samples prepared by conventional granular techniques, where the control over the size and their distributions can hardly be achieved. Therefore, in the present report we would like to focus our study on much better quality materials with extremely narrow distribution of particle size and their separations. The materials of our study focus on Pr- and Gd-substituted $CoFe_2O_4$. The nanoparticle assemblies have been produced by the citrate precursor technique [8] and the structural, microscopic and magnetic properties of the materials have been evaluated as a function of particle size.

The research interest lies on cobalt ferrite-based materials because of their potential applications in high-density information storage and magneto-optical devices [9,10]. This is because of various interesting properties possessed by the materials, e.g. strong anisotropy, high saturation, coercivity etc. However, in order to satisfy the requirements for high density media, the magnetic particles must have reduced size (≈ 10 nm) and uniform distribution. The substitution of rare-earth elements in $CoFe_2O_4$ are promising for their magneto-optical recording applications as they are helpful in reducing the Curie temperature (T_c) compared to pure ferrite [11]. In this report, we have substituted Gd and Pr atoms in $CoFe_2O_4$ in order to induce grain size reduction and their distributions. The variations of magnetic properties as a function of size of the nanoparticles have been investigated.

2. Experimental

The preparations were done by thermal decomposition of mixed metal citrate precursor gels. The materials used were analytical grade $Co(NO_3)_2 \cdot 6H_2O$, $Fe(NO_3)_3 \cdot 9H_2O$ and citric acid (Aldrich, 99.999%). In particular, 2.91 g of $Co(NO_3)_2 \cdot 6H_2O$, 8.08 g of $Fe(NO_3)_3 \cdot 9H_2O$ and 10 g of citric acids were mixed in order to prepare pure cobalt ferrite gel. Pure metallic Gd and Pr_6O_{11} were dissolved in dilute nitric acid solution in the required stoichimetry and added to the sol for the preparation of substituted products. The materials were mixed with stoichiometric ratios in deionized (DI) water and kept at 90°C for 6 h and then evaporated at 100°C till colored floppy gels were formed. The gels were dried overnight at 100°C in order to remove excess water. During the process of drying, the gel swells into the fluffy mass that eventually breaks into brittle flakes. The gel is heat treated in air atmosphere at various temperatures for a time duration of 90 min in order to get the oxide materials, that were later proved to be nano-materials having various grain sizes for $CoFe_2O_4$, $CoGd_xFe_{2-x}O_4$ and $CoPr_xFe_{2-x}O_4$, where $x = 0.1$ and 0.2.

The heat-treated nano-crystal assemblies were investigated by X-ray diffraction (XRD), thermogravimetry (TG), differential thermal analysis (DTA) and magnetic measurements. The XRD patterns were recorded using a diffractometer (model D/max-IIB, Rigaku Co., Tokyo, Japan) in the 2θ range 25–70° using $CuK_{\alpha 1}$ ($\lambda = 1.5405$ Å) radiation. The crystallite sizes were calculated using Scherrer's relationship, $d = K\lambda/B\cos\theta$, where 'd' is the average diameter in Å, 'K' is the shape factor, 'B' is the broadening of the diffraction line measured at half of its maximum intensity

in 'radians', λ is the wavelength of X-rays and θ is the Bragg's diffraction angle. The broadening of the (3 1 1) diffraction line ($2\theta = 36^\circ$) of the ferrite materials was considered after computer fit of the X-ray data using the Gaussian line shape. The broadening of the diffraction line due to reduction of crystallite dimensions, i.e. B, was estimated by the relation, $B^2 = B_m^2 - B_s^2$, where B_m is the measured width of the diffraction line at its half maximum and B_s is the measured breadth of the line for the standard at its half maximum. The line broadening of the standard, i.e. Si having a grain size of several microns, having a diffraction line at the 2θ value 28.39°, was used during the size analysis. Thermal studies were done using simultaneous TG-DTA analysis using SSC 5200 model of Seiko Company. Magnetic measurements were carried out at room temperature using a vibrating sample magnetometer (VSM) with a maximum magnetic field of 2 T.

3. Results and discussions

3.1. Solid-state reactivity

The mechanism of mixed metal citrate precursor decomposition is quite sensitive to the formation of ultrafine single-phase ferrite materials. Fig. 1 shows representative TG and DTA plots of the cobalt iron citrate precursor measured at the heating rate 5°C/min. DTA plot shows three exothermic peaks centered at 131.4°C, 198°C and 290°C. The last peak appears as a broad multi-peaked structure and indicates an overlap of various chemical reactions in the temperature region 220–310°C. We have classified four different regions from the TG curves, i.e. RT–100°C (6.76%), 100–160.3°C (25.57%), 160.3–220°C (41.2%) and 220–310°C (58.01%), where significant weight loss occurs. In the literature some studies are available showing that the presence of free excess citric acid and nitrates complicates the decomposition processes [12]. The decomposition is very complex and proceeds through three to four major processes, which include the removal of water and excess nitrates, decomposition of anhydrous citrate complex and free citric acid through intermediates like aconitate, itaconate, itaconic anhydride and complex carbonates leading to $CoFe_2O_4$ formation. The nature of decomposition processes is very sensitive to the gel structure and heating rate. However, excess citric acid helps in reducing the particle size, as a large number of gases, i.e. CO, CO_2, organic products and water vapor etc., evolves during the decomposition process that helps in inhibiting the particle size growth. However, the formation of acetone dicarboxylate complex ($Co_3Fe_6O_4$-$(C_5H_5O_6)_8$) at 220°C has been reported which decomposes to cobalt ferrite thereafter [12]. The observed weight loss of 58.01% matches well with that of 58.82% for the acetone dicarboxylate decomposition to produce nano-meter sized ferrite materials.

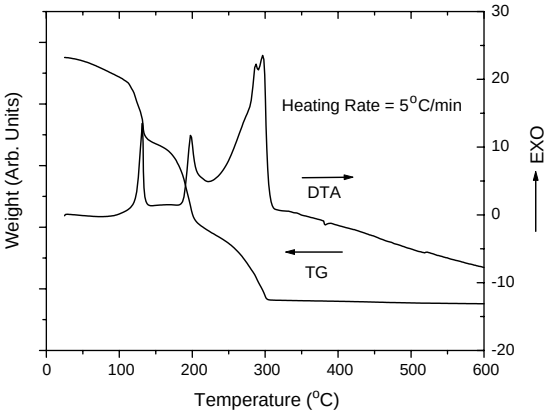

Fig. 1. TG and DTA plots of cobalt iron citrate precursor.

3.2. X-ray diffraction

Fig. 2 shows the XRD patterns of $CoFe_2O_4$ nano-materials synthesized at various temperatures ranging from 300°C to 700°C. All diffraction peaks for the materials correspond to cubic spinel structure. The phase analysis was done with JCPDS card number 22-1086. The XRD lines are broad and the broadening decreases with increasing heat treatment temperatures (Fig. 2). Further, the increase in intensity of X-ray diffraction shows improved crystallinity of the materials. This indicates gradual increase in the crystallite sizes

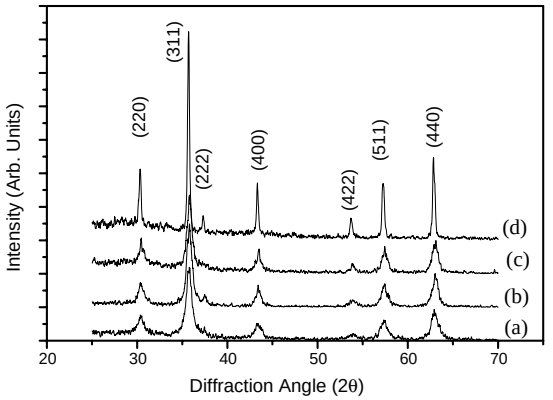

Fig. 2. XRD patterns of pure $CoFe_2O_4$ nano-materials synthesized at various temperatures: (a) 300°C, (b) 400°C, (c) 500°C and (d) 700°C.

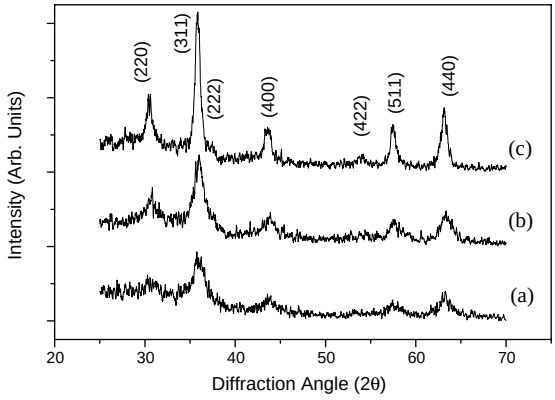

Fig. 4. XRD patterns of $CoPr_{0.1}Fe_{1.9}O_4$ nano-materials synthesized at various temperatures: (a) 300°C, (b) 500°C and (c) 700°C.

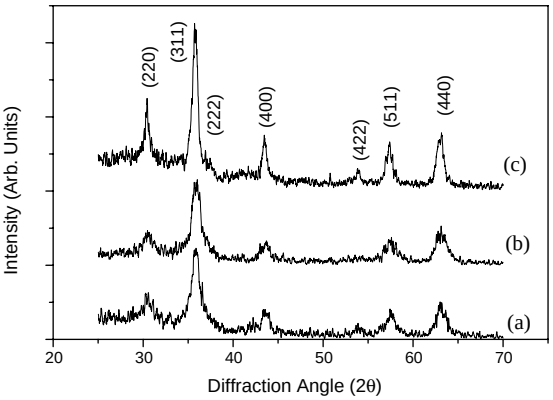

Fig. 3. XRD patterns of $CoGd_{0.1}Fe_{1.9}O_4$ nano-materials synthesized at various temperatures: (a) 300°C, (b) 500°C and (c) 700°C.

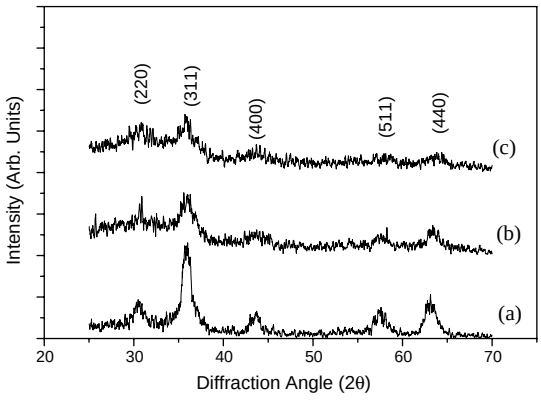

Fig. 5. XRD patterns of $CoGd_xFe_{2-x}O_4$ nano-materials synthesized at 500°C: (a) $x = 0.1$, (b) $x = 0.2$ and (c) $x = 0.3$.

as a function of heat treatment temperatures. Figs. 3 and 4 represent the XRD patterns for $CoGd_{0.1}Fe_{1.9}O_4$ and $CoPr_{0.1}Fe_{1.9}O_4$ nano-materials synthesized at various temperatures, i.e. at 300°C, 500°C and 700°C, respectively. XRD patterns of $CoGd_xFe_{2-x}O_4$, where $0.1 \leqslant x \leqslant 0.3$, synthesized at 500°C are presented in Fig. 5. XRD patterns for $CoRE_{0.1}Fe_{1.9}O_4$ materials are in agreement with those of the pure cobalt ferrites. However, the diffraction peaks in $CoRE_{0.1}Fe_{1.9}O_4$ appear to be broader as a result of incorporation of the rare-earth atoms. Such kinds of results have already been reported in the literature in the study of thin ferrite films [11]. With the gradual increase in rare-earth contents, materials crystallize with more difficulty and some sort of amorphous-like phases prevail. The appearance of significant amorphous-like phase for $CoGd_{0.3}Fe_{1.7}O_4$ in the XRD pattern (Fig. 5(c)) compared with those for lower rare-earth contents (i.e. $x = 0.1$ and $x = 0.2$) (Fig. 5(a) and (b)) confirms the above arguments. We did not detect any extra reflections in the X-ray diffraction patterns corresponding to oxides of Pr or Gd.

Fig. 6 shows the average crystallite sizes as a function of preparation temperature for Pr- and Gd-substituted ferrites along with those for the pure cobalt ferrites. The peak positions for the

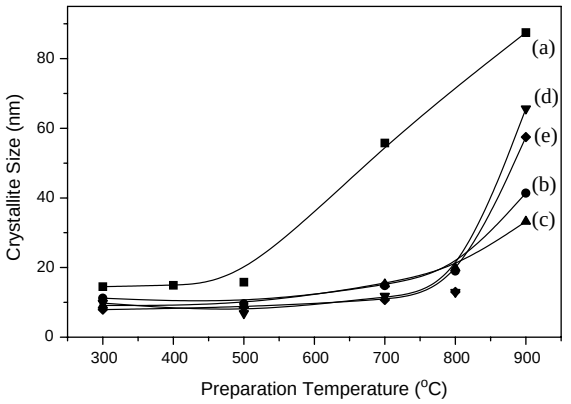

Fig. 6. Plots of crystallite size as a function of preparation temperature: (a) $CoFe_2O_4$ (■), (b) $CoGd_{0.1}Fe_{1.9}O_4$ (●), (c) $CoPr_{0.1}Fe_{1.9}O_4$ (▲), (d) $CoGd_{0.2}Fe_{1.8}O_4$ (▼) and (e) $CoPr_{0.2}Fe_{1.8}O_4$ (◆).

100% intensity peaks of our materials at the 2θ value $\approx 35.8^\circ$ do not vary more than 0.1°, indicating that the effect of lattice strains in XRD line broadening is not significantly large. We have not corrected for the strain broadenings in our analysis. The absence of lattice strains in cobalt ferrite samples prepared by an oxidative precipitation method has already been reported [13]. It can be seen from Fig. 6 that crystallite sizes of pure cobalt ferrite materials synthesized below 500°C are of nanocrystalline nature ($t \approx 15$ nm). The crystallite size increases significantly when the preparation temperature exceeds 500°C. It should be noted that the single-domain size of the cobalt ferrite material is estimated to be 70 nm [14]. This single-domain size for the cobalt ferrite is overcame for materials synthesized at 750°C in our study, and the temperature goes far beyond 900°C for Gd- and Pr-substituted materials. However, it is interesting to note that abnormal grain growth for Pr- and Gd-substituted products become significant after heating above 800°C. Therefore, with Pr and Gd substitution in $CoFe_2O_4$ materials, the grain size is maintained below 15 nm even up to the preparation temperature of 800°C. As the magnetic recording performance of the magnetic materials is improved for well-crystallized materials with nano-dimensions, the effect of rare-earth substitution seems to be extremely valuable in this regard.

3.3. Magnetic properties

A typical hysteresis curve for 15.8 nm $CoFe_2O_4$ materials synthesized at 500°C and a time duration of 1.5 h is shown in Fig. 7. The curve indicates the presence of stable ferrimagnetic fractions of $CoFe_2O_4$ ferrite materials at room temperature. The specific magnetizations measured at room temperature in higher field strengths (i.e. 12–20 kOe) vary almost linearly with $1/H$. The saturation magnetization is estimated from the intercept to the magnetization axis as $1/H$ approaches zero [15]. Fig. 8 shows the estimated values of saturation magnetization as a function of preparation temperatures for the ferrite materials. It can be seen from Fig. 8 that the saturation magnetization values decrease with decreasing crystallite sizes, both for the pure cobalt ferrites as well as the rare-earth substituted ones. The saturation magnetization values for the pure ferrites increase significantly when the materials were synthesized above 500°C. Referring to Fig. 6, the materials synthesized at 500°C are below 18 nm in size and significant grain growth takes place after 500°C. The magnetization values thereafter remain almost flat with respect to the temperature axis. Therefore the single-domain state of the materials exists in the materials synthesized around 700–800°C which corresponds to crystallite sizes of 56–72 nm. The crystallite size range seems to be in good agreement with the literature

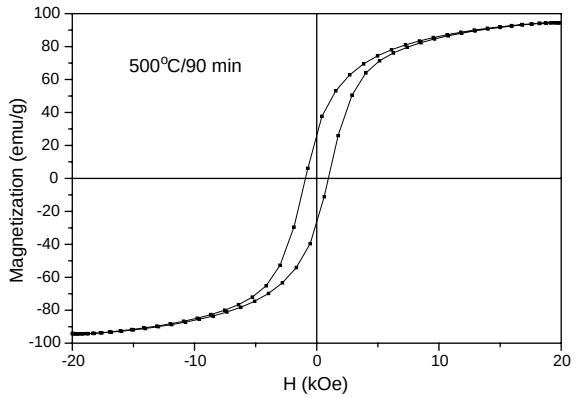

Fig. 7. A typical hysteresis curve for $CoFe_2O_4$ materials synthesized at 500°C and time duration 1.5 h.

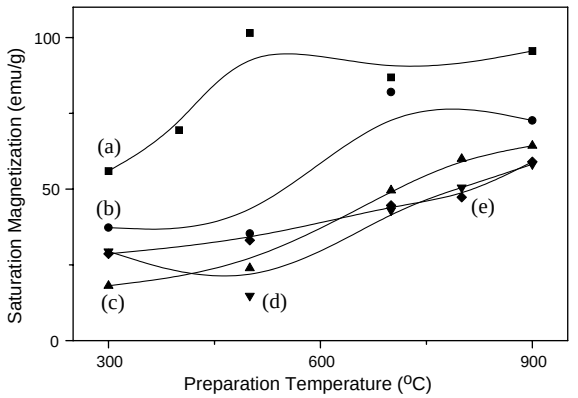

Fig. 8. Plots of saturation magnetization as a function of preparation temperature for the ferrite materials: (a) $CoFe_2O_4$ (■), (b) $CoGd_{0.1}Fe_{1.9}O_4$ (●), (c) $CoPr_{0.1}Fe_{1.9}O_4$ (▲), (d) $CoGd_{0.2}Fe_{1.8}O_4$ (▼) and (e) $CoPr_{0.2}Fe_{1.8}O_4$ (◆).

reported value 70 nm [14]. Substituting Gd and Pr in $CoFe_2O_4$ reduces the saturation magnetization values compared with that of the corresponding pure material. The reductions of magnetic moments in Gd-substituted materials are lesser than those of the Pr-substituted ones. The magnetic moments in the case of the rare-earth ions generally originates from the localized 4f electrons and they are characterized by lower ordering temperatures, i.e. less than 40 K [16]. Therefore, the effect of rare-earth atoms in the cobalt ferrite materials seems to be similar to the substitution of non-magnetic atoms in the octahedral Fe sites of the spinel lattices. As the net magnetic moments in the ferrimagnetic ferrite materials depend on the number of magnetic ions occupying the tetrahedral and octahedral sites, the reduction of magnetization as a function of rare-earth substitution is clear. However, the variations in the size and surface effects of the nano-materials may complicate the above arguments [8,17]. This fact is evident as we observe lower saturation magnetization values for the Gd- and Pr-substituted ferrite materials having smaller crystallite sizes synthesized up to 800°C (Fig. 8(b)–(e)) compared with the pure cobalt ferrite (Fig. 8(a)).

In general, ultrafine particles of magnetic materials are superparamagnetic below a certain critical size and finite temperature. For non-interacting particles with uniaxial magnetic anisotropy, the superparamagnetic relaxation is given by the expression

$$\tau = \tau_0 \exp(KV/kT), \tag{1}$$

where k is the Boltzmann's constant, K is the magnetic anisotropy constant, T is absolute temperature and V is the volume of the particle. It has been shown by room temperature Mossbauer spectroscopy measurements that for $CoFe_2O_4$ crystallites having size less than 12 nm, τ is smaller than the experimental Mossbauer measurement time and the rapid magnetic fluctuations result in net zero magnetic moment of the material leading to superparamagnetic state. However, in our case, due to particle size distribution in the materials, a mixture of superparamagnetic and ferrimagnetic state may exist in the materials. We expect such a situation in our materials as the crystallite size ranges from 9 to 18 nm for pure $CoFe_2O_4$ synthesized below 500°C and Gd- and Pr-substituted $CoFe_2O_4$ synthesized below 800°C. Therefore, the reduction of saturation magnetization values compared with the bulk value, i.e. $\approx$93 emu/g, is majorly due to the thermal effects (superparamagnetism) [18]. In addition, change in the magnetic structure on the surface of the particles is significant, due to large surface/volume ratios of the nano-particles [19]. In order to account for the reduction of saturation magnetization in ultrafine crystallite systems, canted spin structures on the surface layer of each crystallite composing a particle has been proposed [20]. It has been well established in the literature that due to lack of balance exchanged interactions for the magnetic ions on the surface of ultrafine particles, spins are canted on the surface [21].

Fig. 9 shows the variation of coercivities as a function of preparation temperature for the pure (Fig. 9(a)) and rare-earth-substituted ferrite materials (Fig. 9(b)–(d)). The coercivity values for pure $CoFe_2O_4$ materials vary from 0.9 kOe corresponding to 14.5 nm size to 0.7 kOe corresponding to 87.5 nm size. The coercivity values for rare-earth-substituted $CoFe_2O_4$ are smaller than those for pure cases synthesized under similar conditions except for $CoGd_{0.1}Fe_{1.9}O_4$ (Fig. 9(b)). One can see

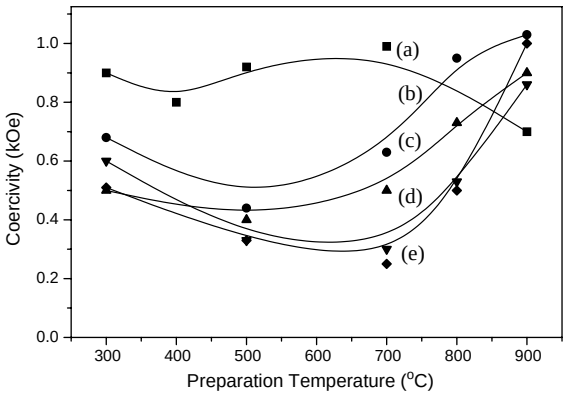

Fig. 9. Variation of coercivity as a function of preparation temperature for the ferrite materials: (a) $CoFe_2O_4$ (■), (b) $CoGd_{0.1}Fe_{1.9}O_4$ (●), (c) $CoPr_{0.1}Fe_{1.9}O_4$ (▲), (d) $CoGd_{0.2}Fe_{1.8}O_4$ (▼) and (e) $CoPr_{0.2}Fe_{1.8}O_4$ (◆).

from Fig. 9 that the coercivity values for the doped materials initially decrease, passes through a minimum and increases thereafter. The minimum shifts towards higher temperature (range 500–700°C) when the rare-earth contents (x) in the ferrite materials increase from 0.1 to 0.2. However, the coercivity values for the rare-earth-doped samples exceed the corresponding values for pure cobalt ferrites for the materials synthesized above 800°C. The crystallite sizes for the $CoGd_{0.1}Fe_{1.9}O_4$, $CoPr_{0.1}Fe_{1.9}O_4$, $CoGd_{0.2}Fe_{1.8}O_4$ and $CoPr_{0.2}Fe_{1.8}O_4$ materials synthesized at 900°C are 41.4, 33.2, 65.6 and 57.5 nm, respectively. Therefore, we conclude that the substitution of rare-earth contents in the cobalt ferrite materials reduces the grain size in a systematic manner and is characterized by improved magnetic properties when the materials are synthesized in the temperature range 800–900°C. This result may be compared with the findings of Cheng et al. [10] where increase of coercivity has been observed by substituting rare-earth atoms (for $x = 0.1$) in the cobalt ferrite thin film materials deposited by a similar method. These effects may be attributed to the contribution from the single ion anisotropy of the rare-earth ions present in the crystal lattice and the surface effects resulting from alteration of the magnetic structures on the surface of the nanoparticles.

4. Conclusions

In the present paper, the magnetic properties of nano-crystalline $CoM_xFe_{2-x}O_4$ (where M = Gd and Pr and $x = 0$, 0.1 and 0.2) powders have been investigated as a function of crystallite size. The effects of incorporating rare-earth atoms in the spinel crystal lattice have been studied in detail. The materials have been synthesized by thermal decomposition of the mixed metal citrate precursors at various temperatures and the crystallite sizes were varied within the range 6.8–87.5 nm. Substitution of rare-earth atoms in the cobalt ferrite materials reduces the grain size of the materials and alters the saturation magnetization and coercivity values to a large extent. We observed improved magnetic characteristics, e.g. saturation magnetization and coercivity, in Gd- and Pr-substituted ferrites when prepared in the temperature range 800–900°C. The experimental results have been explained on the basis of size and surface effects of the ultrafine materials and the alteration of the magnetic structures due to the contribution from the single ion anisotropy of the rare-earth ions present in the crystal lattice.

Acknowledgements

The authors are grateful for the sponsorship of this research in part by the National Science Council of the Republic of China, under the grant NSC89-2216-E007-081.

References

[1] H.J. Richter, J. Phys. D: Appl. Phys. 32 (1999) R147.
[2] H. Gleiter, J. Weissmuller, O. Wollersheim, R. Wurschum, Acta Mater. 49 (2001) 737.
[3] J.P. Chen, et al., Phys. Rev. B 54 (1996) 9288.
[4] R.N. Panda, N.S. Gajbhiye, J. Appl. Phys. 81 (1997) 335.
[5] S. Morup, E. Tronc, Phys. Rev. Lett. 72 (1994) 3278.
[6] J.L. Dormann, L. Bessasis, D. Fiorani, J. Phys. C 21 (1988) 2015.
[7] J.M. de Teresa, A. Barthelemy, J.P. Contour, A. Fert, J. Magn. Magn. Mater. 211 (2000) 160.
[8] S. Prasad, N.S. Gajbhiye, J. Alloys Compounds 265 (1998) 87.
[9] M.H. Kryder, MRS Bull. 21 (1996) 17.

[10] F. Cheng, C. Liao, J. Kuang, Z. Xu, C. Yan, L. Chen, H. Zhao, Z. Liu, J. Appl. Phys. 85 (1999) 2782.
[11] F. Cheng, J. Jia, Z. Xu, B. Zhou, C. Liao, L. Chen, H. Zhao, J. Appl. Phys. 86 (1999) 2727.
[12] N.S. Gajbhiye, S. Prasad, Thermochim. Acta 285 (1996) 325.
[13] M. Rajendran, R.C. Pullar, A.K. Bhattacharya, D. Das, S.N. Chintalapudi, C.K. Majumdar, J. Magn. Magn. Mater. 132 (2001) 71.
[14] A. Berkowitz, W.T. Schuele, J. Appl. Phys. 30 (1959) 134S.
[15] C.P. Bean, I.S. Jacobs, J. Appl. Phys. 31 (1960) 1228.
[16] W.J. Nellis, S. Legvold, Phys. Rev. 180 (1969) 581.
[17] A.T. Ngo, P. Bonville, M.P. Pileni, J. Appl. Phys. 89 (2001) 3370.
[18] S. Ammar, A. Helfen, N. Jouini, F. Fievet, I. Rosenman, F. Villain, P. Molinie, M. Danot, J. Mater. Chem. 11 (2001) 186.
[19] K. Haneda, Can. J. Phys. 65 (1987) 1233.
[20] A.H. Morrish, K. Haneda, J. Magn. Magn. Mater. 35 (1983) 105.
[21] J.M.D. Coey, Phys. Rev. Lett. 27 (1971) 1140.